2013 European Control Conference (ECC)
July 17-19, 2013, Zürich, Switzerland.

Hysteresis Compensation and Adaptive LQR Design for an Electro-Pneumatic Clutch for Heavy Trucks

Harald Aschemann, Robert Prabel and Dominik Schindele

Abstract— **In this paper, a nonlinear model-based control design for an electro-pneumatic clutch for heavy trucks is presented. A clutch is required at start-up or during gear shifts to disconnect the combustion engine from the gear box. This automated actuator disburdens the driver and provides the necessary actuation force. The proposed feedback control represents an adaptive LQR design using extended linearisation techniques, where the controller gains are adapted by solving numerically the corresponding Riccati equation in real-time. In addition, an adaptive feedforward control is designed with the clutch position as controlled variable. The control structure is extended by a reduced-order observer that estimates an effective pressure, which accounts for model uncertainty as well as nonlinear friction. Moreover, an experimentally identified Bouc-Wen hysteresis model is used to improve the dynamic behaviour further. Thereby, high tracking accuracy is achievable for the piston position. The performance of the proposed control structure is pointed out by experimental results from a dedicated test rig.**

I. INTRODUCTION

Clutches are needed in vehicle power trains to decouple the angular velocities of the internal combustion engine from those of the driving wheels. Especially at start-up, when the velocity of the vehicle is zero, and during the gear shift process the clutch has to be employed. Due to the large torque transmitted through the clutch, an electro-pneumatic actuator is advantageously used in truck applications. Often, the clutch operation is automated using a combination of feedforward and feedback control, e.g., nonlinear control approaches as presented in [1], [2], and [3]. A test rig dedicated for the development and validation of sophisticated control approaches for an electro-pneumatic clutch is in place at the Chair of Mechatronics at the University of Rostock, see Fig. 1. An overview of the adaptive LQR design with state-dependent matrices is given in [4] and [5].

The single disc dry clutch under consideration is driven by the piston rod of a pneumatic cylinder, which is actuated by pressurised air. Due to safety specifications, it is necessary to employ two inlet and two outlet valves, typically with different conductances. These electrically actuated valves operate in an on/off mode using a pulse-width-modulated signal (PWM). In truck applications, the only measured state variable is usually the position of the piston in the pneumatic cylinder. The velocity of the piston can be calculated by real differentiation. The internal pressure in the piston chamber, however, has usually to be determined by a state observer as discussed in [6], [7]. For an experimental identification of the system the test rig has been equipped with additional sensors not present in the real truck: a sensor for the internal pressure, a force transducer, and a mass flow sensor for the supply air mass flow. With this sensor combination, an accurate identification of the system parameters and the component characteristics becomes possible.

Harald Aschemann, Robert Prabel and Dominik Schindele are with the Chair of Mechatronics, University of Rostock, Germany. {Harald.Aschemann, Robert.Prabel, Dominik.Schindele}@uni-rostock.de

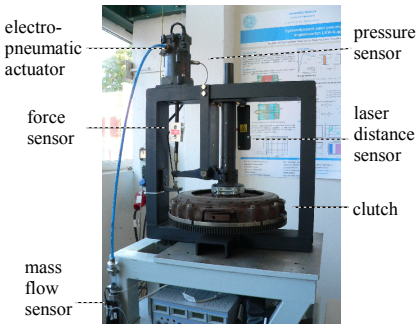

Fig. 1. Test rig for the electro-pneumatic clutch.

This paper is organized as follows: in Sec. II, a control-oriented state-space model of the mechatronic system is derived. This includes a Bouc-Wen hysteresis model that is identified for the mechanical subsystem. The adaptive feedback and feedforward control design based on extended linearisation techniques is presented in Sec. III. Furthermore, a nonlinear reduced-order observer is designed and implemented that estimates an effective pressure in the cylinder that also accounts for a lumped disturbance variable, see Sec. IV. In Sec. V, the obtained experimental results show the advantages of the proposed control approach with small tracking errors during transient phases as well as a negligible steady-state control error.

II. MODELLING OF THE MECHATRONIC SYSTEM

The mechatronic system can be split into a mechanical and a pneumatic subsystem. The mechanical system part covers the motion of the piston. The pneumatic subsystem describes the pressure dynamics in the pneumatic cylinder. The flow characteristics of the on/off valves in combination with pulse-width-modulation determines the in-flowing and out-flowing air mass flows.

A. Mechanical Subsystem

The considered operation range of the system – around the biting point, where the clutch allows for a torque transmission – is characterised by positive values $0 < z(t) < l_{max}$, cf. Fig. 2. The equation of motion for the piston rod follows

directly from a force balance. The force of an internal return

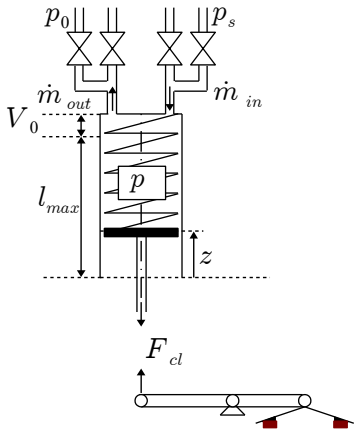

Fig. 2. Mechatronic model of the electro-pneumatic clutch.

spring is given by $F_{sp}(t) = c_{sp}\,(z_{sp} + z(t))$, where the value z_{sp} denotes the initial pre-load. A movement in the positive z-direction, hence, results in a linear increase in the restoring force of this spring. The overpressure $p_z(t) = p(t) - p_0$, which represents the difference between the absolute pressure $p(t)$ and the ambient pressure p_0, leads to a corresponding force on the piston according to $F_p(t) = -A_k\, p_z(t)$. Here, A_k stands for the piston sectional area. The characteristic of the main clutch force is nonlinear and subject to hysteresis. For modelling, the clutch force is divided into a static part $F_{cl,st}(z)$ as medium curve and a hysteresis part $F_{cl,hys}(z,\xi)$

$$F_{cl}(z,\xi) = F_{cl,st}(z) + F_{cl,hys}(z,\xi)\,. \tag{1}$$

The static clutch characteristic has been identified experimentally and approximated by a sixth-degree polynomial ansatz function for the mean value of the opening clutch force $F_{cl,o}(z)$ as well as the closing clutch force $F_{cl,c}(z)$ at a given position $z(t)$

$$F_{cl,st}(z) = \frac{1}{2}\left(F_{cl,o}(z) + F_{cl,c}(z)\right) = \sum_{i=0}^{6} p_{i,st}\, z^i\ . \tag{2}$$

The hysteresis part of the clutch force as deviation from the medium curve $F_{cl,st}(z)$ is modelled by the generalised Bouc-Wen-model $F_{cl,hys} = F_{cl,hys}(z,\xi)$ as described in the next subsection.

Model uncertainty as well as damping and nonlinear friction could be advantageously taken into account by a lumped disturbance force $F_U(t)$. A balance of momentum yields the equation of motion in the form of a second order differential equation

$$\begin{aligned}\ddot{z}(t) = \frac{1}{m}[&-A_k p_z(t) - c_{sp}(z_{sp} + z(t)) \\ &+ F_{cl,st}(z) + F_{cl,hys}(z,\xi)) - F_U(t)]\,,\end{aligned} \tag{3}$$

with m as the reduced mass of all the moving components of the pneumatic clutch.

B. Bouc-Wen Hysteresis Model

In previous work, the hysteresis force was described by an additional switching term in the form of a signum-function, cf. [1] and [8]. This static hysteresis modelling, however, has the main drawback that the hysteresis is zero for a vanishing piston velocity $\dot{z} = 0$. A further drawback is given by frequent switchings of the sign-function that result in the case of a noisy signal for the piston velocity. A suitable countermeasure is the approximation of the sign-function by the following regularised function $\mathrm{sign}(\dot{z}) \approx \tanh(\frac{\dot{z}}{\varepsilon})$, $\varepsilon \ll 1$. As a refined hysteresis model, in this contribution a generalised Bouc-Wen model is employed. It is able to cover the most significant hysteresis effects. As this dynamic hysteresis model is characterised by only one additional differential equation, it is well suited for implementation in simulations or real-time applications. Whereas the classical Bouc-Wen model [9] is not able to describe asymmetric hysteresis loops, the generalised Bouc-Wen model, proposed in [10], solves this problem. The generalised Bouc-Wen model for the clutch force hysteresis can be stated by the following output equation

$$F_{cl,hys}(z,\xi) = \alpha\ k_0\ z + (1-\alpha)\ k_0\ \xi\ , \tag{4}$$

in combination with a first order differential equation for an additional dimensionless internal state variable ξ

$$\dot{\xi}(z,\dot{z},\xi) = \dot{z}[A - |\xi|^n\ \psi(z,\dot{z},\xi)]\,. \tag{5}$$

Here, α and k_0 represent stiffness parameters, whereas A and n denote parameters that determine the scale and the sharpness of the hysteresis loop. In this paper, the parameter n is fixed to $n = 1$. The nonlinear function $\psi(z,\dot{z},\xi)$ can be used to specify further shape characteristics. For the generalised Bouc-Wen model, the shape-control function ψ is chosen as follows

$$\begin{aligned}\psi(z,\dot{z},\xi) \quad = \quad &\beta_1\,\mathrm{sign}(\dot{z}\xi) + \beta_2\,\mathrm{sign}(z\dot{z}) + \beta_3\,\mathrm{sign}(z\xi) \\ &+\beta_4\,\mathrm{sign}(\dot{z}) + \beta_5\,\mathrm{sign}(\xi) + \beta_6\,\mathrm{sign}(z)\ ,\end{aligned} \tag{6}$$

with six parameters $\beta_i,\ i = 1,\ldots,6$, determining the shape of the curve. Thereby, the hysteresis curve is divided in six

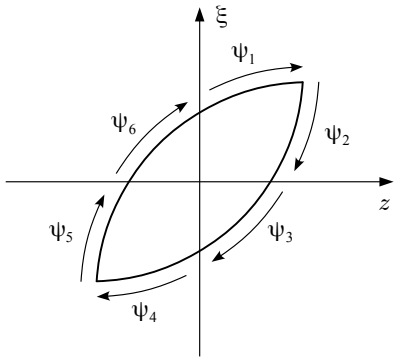

Fig. 3. Different phases of the hysteresis loop for the generalised Bouc-Wen model.

different phases, which depend on different combinations of the signs of z, $\dot{z}$ and ξ. The separate phases $\psi_i,\ i = 1,\ldots,6$

of the shape-control function are depicted in Fig. 3. The linear relationship between the parameters ψ_i and β_i can be represented by the following matrix

$$\begin{bmatrix}\psi_1\\ \psi_2\\ \psi_3\\ \psi_4\\ \psi_5\\ \psi_6\end{bmatrix} = \begin{bmatrix} 1 & 1 & 1 & 1 & 1 & 1\\ -1 & -1 & 1 & -1 & 1 & 1\\ 1 & -1 & -1 & -1 & -1 & 1\\ 1 & 1 & 1 & -1 & -1 & -1\\ -1 & -1 & 1 & 1 & -1 & -1\\ 1 & -1 & -1 & 1 & 1 & -1\end{bmatrix} \begin{bmatrix}\beta_1\\ \beta_2\\ \beta_3\\ \beta_4\\ \beta_5\\ \beta_6\end{bmatrix}. \quad (7)$$

With α, A, k_0 and $\beta_1,....,\beta_6$, the generalised Bouc-Wen model involves nine unknown parameters, which can be identified by optimisation techniques. Here, an evolutionary optimisation routine is employed, cf. [12].

C. Pneumatic Subsystem

The dynamics of the internal pressure follows directly from a mass flow balance in combination with a polytropic change of thermodynamic state for the compressed air in the cylinder chamber. As the supply pressure p_S is at a value of approx. $p_S = 9$ bar, the ideal gas equation represents an accurate description of the thermodynamic behaviour of the compressed air

$$\frac{p(t)}{\rho(t)} = R_L \cdot T(t). \quad (8)$$

Here, the density $\rho(t)$, the gas constant of air R_L and the thermodynamic temperature $T(t)$ are introduced. The thermodynamic process is modelled as a polytropic change of state according to $p(t)\cdot\rho^{-n}(t) = \text{const.}$, where $n = 1.2$ denotes the identified polytropic exponent. The polytropic exponent is, hence, in the range between $n = 1$ for an isothermal process and $n = \kappa$ for an isentropic process. The relationship between the time derivative of the pressure $p(t)$ and the time derivative of the density $\rho(t)$ results in

$$\dot{p}(t) = \dot{p}_z(t) = nR_L T(t)\dot{\rho}(t). \quad (9)$$

The mass balance for the cylinder is governed by

$$\dot{\rho}(t)V(t) = \dot{m}(t) - \rho(t)A_k\dot{z}(t), \quad (10)$$

where $V(z(t)) = V_0 + A_k(l_{max} - z(t))$ denotes the total volume of the cylinder chamber. By inserting (9) in the mass balance (10), the first-order differential equation for the cylinder pressure results in

$$\dot{p}(t) = \dot{p}_z(t) = \frac{nR_L T(t)\dot{m}(t)}{V(z(t))} + \frac{(p_z(t)+p_0)nA_k\dot{z}(t)}{V(z(t))}, \quad (11)$$

where $\dot{m}(t)$ denotes the total mass flow of air provided by the inlet and outlet valves. The internal temperature $T(t)$ can be approximated with good accuracy by the constant temperature T_{amb} of the ambiance. In this way, temperature measurements can be avoided, and the implementation effort is significantly reduced. To simplify the control design, the term $u(t) = R_L \cdot T_{amb} \cdot \dot{m}(t)$ is introduced as control input.

D. Valve Actuation

The main advantage of on/off valves is that they are more energy efficient than proportional valves. To actuate this type of valve proportionally, a pulse-width-modulated signal (PWM) is necessary. The PWM-signal is calculated by a comparison of the continuous signal with a saw-tooth-signal. Instead of using the PWM-signal and mathematical description for the mass flow, an experimental identification of the mass flow characteristic has been carried out, see [8] for details. A corresponding approximative inverse can be derived numerically with high accuracy. A pre-multiplication with this inverse valve characteristic, see Fig. 5, practically eliminates the dead zone behaviour as well as linearises the nonlinear valve characteristic.

III. Adaptive Control Design Using Extended Linearisation Techniques

In the following, the feedforward and feedback control design using extended linearisation will be presented. Note that the lumped disturbance force $F_U(t)$ is not considered here but counteracted separately by the estimated effective pressure from a reduced-order observer, see section IV. For the extended linearisation, the right hand side of the nonlinear state equation is written in quasi-linear form with state-dependent matrices

$$\underline{f}(\underline{x},\xi,u) = \underline{A}(z(t),\dot{z}(t),\xi(t))\underline{x}(t) + \underline{b}(z(t))u(t). \quad (12)$$

Here, the system matrix $\underline{A}(z,\dot{z},\xi(t))$ and the vector $\underline{b}(z)$ depend on the measurable state variables piston position $z(t)$ and piston velocity $\dot{z}(t)$ as well as on the reconstructed internal state variable $\xi(t)$ of the generalised Bouc-Wen model

$$\dot{\underline{x}}(t) = \begin{bmatrix} 0 & 1 & 0\\ -\dfrac{c_{sp}(z+z_{sp})}{mz} + \dfrac{F_{cl}(z,\xi)}{mz} & 0 & -\dfrac{A_k}{m}\\ 0 & \dfrac{np_0A_k}{V(z)} & \dfrac{n\dot{z}A_k}{V(z)}\end{bmatrix}\underline{x}(t) + \begin{bmatrix}0\\0\\ \dfrac{n}{V(z)}\end{bmatrix}u(t), \quad \underline{x}(t) = \begin{bmatrix}z(t)\\ \dot{z}(t)\\ p_z(t)\end{bmatrix}. \quad (13)$$

Please note that the dominant nonlinear terms like the hysteresis force $F_{cl}(z(t),\xi(t))$ are included exactly in the right hand side. Obviously, alternative decompositions (12) are possible that lead to different state-depending matrices. In the considered operating range, a position value within the interval $0 < z(t) < l_{max}$ is guaranteed such that the singularities are avoided and, hence, are not critical. The state-dependent representation according to (13) leads to nonlinear expressions for the control gains that are adapted to the chosen scheduling variables.

A. Adaptive LQR Design

The design of the state feedback for the electro-pneumatic clutch is carried out on the basis of the LQR approach, where the vector of feedback gains is determined by minimisation of a quadratic cost function with a combined weighting of the state variables as well as the control inputs. The control gains follow from a numerical online-solution of the corresponding algebraic Riccati equation (ARE). Due to the dependency of the system matrices on the state variables position $z(t)$, velocity $\dot{z}(t)$, and the internal state variable of the Bouc-Wen hysteresis model $\xi(t)$, the ARE becomes also a function of these scheduling variables. The starting point for the LQR design is the time-weighted cost function

$$J = \frac{1}{2}\int_0^\infty \left[\underline{x}^T \underline{Q}\underline{x} + ru^2\right] e^{2\alpha t} dt\,, \tag{14}$$

which contains the constant weighting matrix $\underline{Q}$, the scalar weight r, and an additional parameter α. The weighting matrix $\underline{Q}$ for the state vector $\underline{x}$ is chosen as a positive definite diagonal matrix $\underline{Q} > 0$, the scalar input weight as a constant positive value $r = 1$. The positive parameter $\alpha > 0$ defines a stability margin of the closed-loop eigenvalues s_i, $i = \{1,2,3\}$, according to

$$\max_i \{Re(s_i)\} \leq -\alpha\,. \tag{15}$$

In the s-plane, hence, all closed-loop eigenvalues s_i are located left to a parallel line at the distance α from the imaginary axis. In each operating point, characterised by $z(t)$, $\dot{z}(t)$ and $\xi(t)$, the optimal feedback control law can be determined as the positive definite solution $\underline{P} = \underline{P}(z,\dot{z},\xi)$ of the parameter-dependent ARE

$$\underline{A}_\alpha^T(z,\dot{z},\xi)\underline{P} + \underline{P}\underline{A}_\alpha(z,\dot{z},\xi) - r^{-1}\underline{P}\underline{b}(z)\underline{b}^T(z)\underline{P} + \underline{Q}(z) = \underline{0}\,. \tag{16}$$

The ARE is solved online using the iterative algorithm proposed by Kleinman [11]. Based on this algorithm, hence, a symbolic description of a corresponding Lyapunov equation has been derived that is to be solved in each iteration step. In the real-time implementation only a fixed number of iterations are performed. As initialisation the solution of the previous time step is used. The parameter-dependent state feedback with $k_{Ri} = k_{Ri}(z,\dot{z},\xi)$ becomes

$$u_{FB} = -\underline{k}^T(z,\dot{z},\xi)\,\underline{x} = -[k_{R1}\,k_{R2}\,k_{R3}]\,\underline{x}\,, \tag{17}$$

with the vector of feedback gains

$$\underline{k}^T(z,\dot{z},\xi) = r^{-1}\underline{b}^T(z)\underline{P}(z,\dot{z},\xi)\,. \tag{18}$$

The matrix $\underline{A}_\alpha$ used in the ARE is related to the system matrix $\underline{A}$ according to

$$\underline{A}_\alpha(z,\dot{z},\xi) = \underline{A}(z,\dot{z},\xi) + \alpha\underline{I}_3\,. \tag{19}$$

As the system matrix $\underline{A}_\alpha(z,\dot{z},\xi)$ depends continuously on the three scheduling variables and as a constant weighting matrix $\underline{Q}$ as well as a constant input weight r are employed, the solutions $\underline{P}(z,\dot{z},\xi)$ of the ARE are continuous functions as well. The same applies to the vector of feedback gains. As shown in Fig. 4, the dimensionless internal state variable $\xi(t)$ remains bounded. The favourable stability properties of the adaptive LQR design regarding locally asymptotic stability of the time-varying system are discussed in [4].

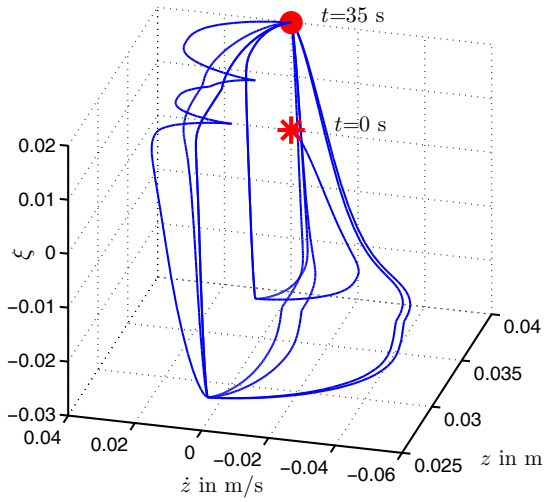

Fig. 4. Boundedness of the internal state variable of the generalised Bouc-Wen model in the experiments presented in Sec. V.

B. Adaptive Feedforward Control Design

For feedforward control design, the position of the clutch $y(t) = z(t)$ is considered as the controlled variable. Thus, the linear output equation is given by

$$y(t) = \begin{bmatrix} 1 & 0 & 0 \end{bmatrix} \underline{x}(t) = \underline{c}^T\,\underline{x}(t)\,. \tag{20}$$

The control transfer function can be calculated as

$$\frac{Y(s)}{U_{FF}(s)} = \underline{c}^T\left(s\underline{I} - \underline{A} + \underline{b}\underline{k}^T\right)^{-1}\underline{b} = \frac{b_0}{N(s)}\,. \tag{21}$$

Obviously, the numerator of the control transfer function contains no transfer zero. The main idea of the feedforward control design is the modification of the numerator of the control transfer function by introducing a polynomial ansatz for the feedforward control action in the Laplace domain according to

$$U_{FF}(s) = \left[k_{V0} + k_{V1}\cdot s + k_{V2}\cdot s^2 + k_{V3}\cdot s^3\right] Y_d(s)\,. \tag{22}$$

For its realisation the desired trajectory $y_d(t) = z_d(t)$ as well as the first three time derivatives are available from a state variable filter. The feedforward gains can be computed from a comparison of the corresponding coefficients in the numerator as well as the denominator polynomials of

$$\frac{Y(s)}{Y_d(s)} = \frac{b_0\cdot\left[k_{V0} + \ldots + k_{V3}\cdot s^3\right]}{a_0 + a_1\cdot s + a_2\cdot s^2 + s^3}$$

according to $a_i = b_0\cdot k_{Vi}, i = 0,\ldots,n = 3$. This leads to the following feedforward gains depending both on the desired values z_d as well as $\dot{z}_d$ and on the internal state variable ξ

of the Bouc-Wen model

$$k_{V0} = k_{V0}(z_d, \dot{z}_d, \xi), \tag{23}$$

$$k_{V1} = -p_0\, A_k + k_{R2}(z_d, \dot{z}_d, \xi) \tag{24}$$

$$- \frac{c_{sp}(z_{sp} + z_d) - V(z_d)\, F_{cl}(z_d, \xi)}{A_k\, n\, z_d}, \tag{25}$$

$$k_{V2} = m\, \dot{z}_d - \frac{m\, k_{R3}(z_d, \dot{z}_d, \xi)}{A_k}, \tag{26}$$

$$k_{V3} = -\frac{m\, V(z_d)}{A_k\, n}. \tag{27}$$

IV. Nonlinear Reduced-Order Observer

In truck applications, the pressure $p(t)$ is usually not measured. Unfortunately, it is not possible to design an observer that estimates both the internal pressure p and the lumped disturbance force F_U – affecting the equation of motion (3) – separately. In the following, hence, a nonlinear reduced-order observer according to [12] is designed for the estimation of an effective pressure. Using this estimated effective pressure in the feedback control law, see the block diagram of the implementation in Fig. 5, steady-state accuracy is achieved as shown below. The observer design is based on the nonlinear state space representation (13). The state equations are split into the differential equation for the pressure $y_1(t) = p(t) = p_z(t) + p_0$ to be estimated and the differential equations corresponding to the measurable vector $\underline{y}_2(t) = [z(t), \dot{z}(t)]^T$. This leads to the state-space representation

$$\dot{y}_1 = f_1(y_1, \underline{y}_2, u)\,,\ \dot{\underline{y}}_2 = \underline{f}_2(y_1, \underline{y}_2)\,. \tag{28}$$

The unknown state variable to be estimated is obtained from

$$\hat{y}_1 = \underline{h}^T \cdot \underline{y}_2 + \eta\ , \tag{29}$$

with the observer gain vector $\underline{h}^T = [h_1, h_2]$. The state equation for η is given by

$$\dot{\eta} = \Phi(\hat{y}_1, \underline{y}_2, u)\,. \tag{30}$$

The observer gain vector $\underline{h}^T$ and the nonlinear function Φ have to be chosen properly, so that the steady-state observer error $e(t) = y_1 - \hat{y}_1(t)$ converges to zero. Considering the steady-state condition

$$\dot{e} = 0 = \dot{y}_1 - \underline{h}^T \cdot \dot{\underline{y}}_2 - \Phi(y_1 - 0, \underline{y}_2, u)\ , \tag{31}$$

directly leads to the function $\Phi = \Phi(y_1, \underline{y}_2, u)$. Aiming at an asymptotically stable linearised error dynamics, the eigenvalue of the scalar Jacobian

$$J_e = \left.\frac{\partial \Phi(y_1, \underline{y}_2, u)}{\partial y_1}\right|_{y_1 = \hat{y}_1} = \frac{n \cdot A_k \cdot \dot{z}}{V(z)} + \frac{h_2 \cdot A_k}{m}\,, \tag{32}$$

which is evaluated for $y_1 = \hat{y}_1$, is specified as a real eigenvalue $s_B < 0$. The corresponding observer gain h_2 results in

$$h_2 = \frac{(-n \cdot A_k \cdot \dot{z} + s_B \cdot V(z)) \cdot m}{V(z) \cdot A_k}\,, \tag{33}$$

whereas the observer gain h_1 could be chosen arbitrarily, e.g. as $h_1 = 0$. Evaluating the function $\Phi(\hat{y}_1, \underline{y}_2, u)$ with the estimated pressure $\hat{y}_1 = \hat{p}(t)$, the error dynamics of the observer – now in presence of an unknown lumped disturbance force $F_U(t)$ – becomes

$$\dot{e} = \dot{y}_1 - \underline{h}^T \dot{\underline{y}}_2 - \Phi\left(\hat{y}_1, \underline{y}_2, u\right) = \left[\frac{n A_k \dot{z}}{V(z)} + \frac{h_2 A_k}{m}\right] e + \frac{h_2}{m} F_U\ . \tag{34}$$

Solving (34) for $\hat{p}$ and substituting for h_2 with (33) yields

$$\hat{p} = p - \frac{n \dot{z}}{s_B V(z)} F_U + \frac{1}{A_k} F_U\ . \tag{35}$$

This shows clearly that the nonlinear reduced-order observer provides an estimation of an effective pressure accounting for the disturbance force F_U. In steady-state, where the piston velocity vanishes ($\dot{z} = 0$), the estimated pressure complies exactly with the increased pressure level that is necessary to overcome the lumped disturbance force. The additional term $-\frac{n\dot{z}}{s_B V(z)} F_U$ in the general case with $\dot{z} \neq 0$ is negligible for large values of $|s_B|$. The stability of the closed-loop control system has been investigated thoroughly by simulations.

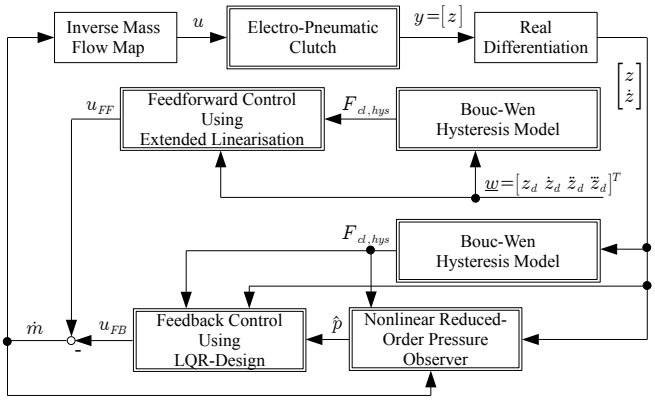

Fig. 5. Block diagram of the control structure.

V. Experimental Results

The following experimental results have been obtained at a

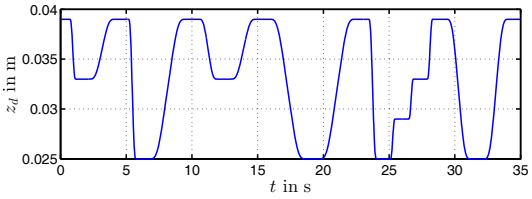

Fig. 6. Desired trajectory for the clutch position.

dedicated test rig for electro-pneumatic clutches at the Chair of Mechatronics at the University of Rostock. In Fig. 6, the desired trajectory $z_d(t)$ for the piston position is depicted. The desired trajectory starts at $z = 0.039$ m. At this position value, the clutch is fully closed and, hence, the power of the combustion engine could be transmitted through the drive train to the gear box. In the following, a sequence of desired motions in the opening and closing directions of the clutch are specified. Here, both intermediate positions corresponding to a sliding clutch and a maximum position

value of $z = 0.026$ m, where the clutch is fully open and does not transmit any torque, are investigated. Fig. 7 shows the

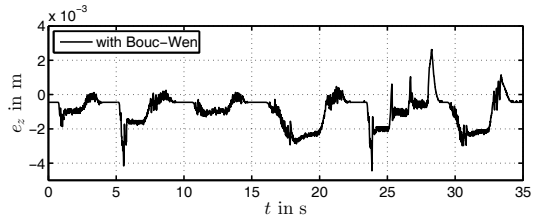

(a) Position error using the measured internal pressure

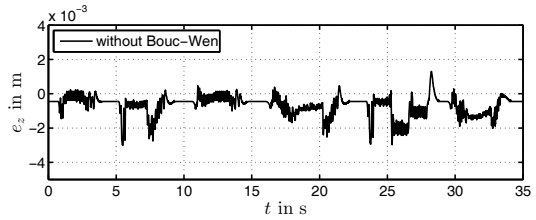

(b) Position error using the measured internal pressure and the Bouc-Wen hysteresis model

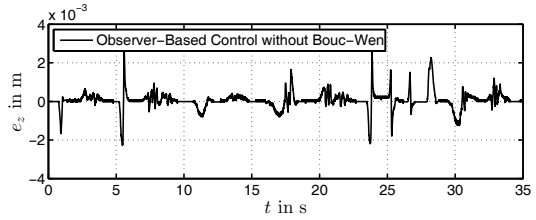

(c) Position error using the estimated effective pressure

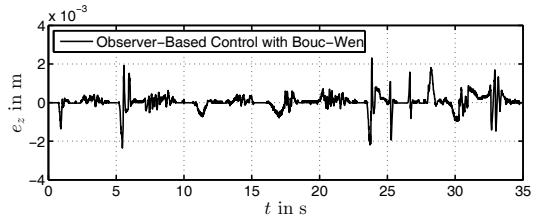

(d) Position error using the estimated effective pressure and the Bouc-Wen hysteresis model

Fig. 7. Tracking error for different control approaches.

obtained tracking errors for four approaches using a sample time of $T_s = 10$ ms in the control implementation: Obviously, the smallest maximum tracking errors of below 2 mm are obtained with the observer-based control approaches depicted in (c) and (d). The corresponding steady-state errors are below 0.2 mm. The extension with the Bouc-Wen model yields slightly smaller errors in (d). Measured values for the internal pressure lead to a significant increase in both the steady-state errors and the tracking errors as depicted in (a) and (b). However, the errors obtained in (a) can be reduced by using the Bouc-Wen model in (b). The corresponding root mean square (RMS) errors for the clutch position $e_{RMS} = \sqrt{\frac{1}{N}\sum_{i=1}^{N}\left(z_d(i) - z(i)\right)^2}$ are shown in Table I. As discussed before, the best results are obtained for the observer-based adaptive LQR feedback in combination with the hysteresis compensation.

LQR	LQR with BW	LQR with Obs.	LQR with Obs. and BW
1.31 mm	0.90 mm	0.44 mm	0.39 mm

TABLE I

ROOT MEAN SQUARE ERROR OF THE CLUTCH POSITION

VI. CONCLUSIONS

This paper presents a model-based approach to tracking control of an electro-pneumatic clutch used in truck applications. The control-oriented model accounts for the dynamic behaviour of the clutch piston as well as the internal pressure in the cylinder chamber. The tracking control design is performed by extended linearisation techniques based on a quasi-linear state-space representation. A combined adaptive feedforward control and LQR feedback is designed, where the algebraic Riccati equation is solved in real-time using the iterative Kleinman-algorithm. The estimation of an effective pressure makes a pressure measurement unnecessary and counteracts model uncertainties as well as friction. Additionally, a generalised Bouc-Wen model is employed for a compensation of hysteresis in the clutch characteristic. The control performance of the proposed control structure is demonstrated by experimental results from an implementation on a dedicated test rig at the Chair of Mechatronics, University of Rostock. The obtained maximum steady-state position errors are below $e_1 = 0.2$ mm for the observer-based control structures.

REFERENCES

[1] H. Aschemann, R. Prabel, and D. Schindele, "Nonlinear control of an electro-pneumatic clutch for truck applications using extended linearisation techniques," *Proc. of 12th Scandin. Intern. Conf. on Fluid Power, SICFP 2011, Tampere, Finland*, 2011.

[2] H. Langjord, T. A. Johansen, and J. P. Hespanha, "Switched control of an electropneumatic clutch actuator using on/off valves," *American Control Conference*, pp. 1513–1518, 2008.

[3] G. O. Kaasa and M. Takahashi, "Adaptive tracking control of an electro-pneumatic clutch actuator," *Modeling, Identification and Control*, vol. 24, no. 4, pp. 217–229, 2003.

[4] T. Çimen, "State-dependent riccati equation (sdre) control: a survey," in *Proceedings of the 17th World Congress, The Interational Federation of Automatic Control*, 2008, pp. 3761–3775.

[5] J. R. Cloutier, "State-dependent riccati equation techniques: an overview," in *American Control Conference, 1997. Proceedings of the 1997*, vol. 2. IEEE, 1997, pp. 932–936.

[6] G. O. Kaasa, *Nonlinear output-feedback control applied to electro-pneumatic clutch actuation in heavy-duty trucks*. Norwegian University of Science and Technology: PhD dissertation, 2006.

[7] H. Langjord, G. O. Kaasa, and T. A. Johansen, "Nonlinear observer and parameter estimation for electropneumatic clutch actuator," *IFAC Symposium on Nonlinear Control Systems*, vol. 8, pp. 789–794, 2010.

[8] H. Aschemann, R. Prabel, and D. Schindele, "Observer-based backstepping control of an electro-pneumatic clutch," *Proceedings of the American Control Conference, Montreal, Canada*, 2012.

[9] Y. Wen, "Method of random vibration of hysteretic systems," *Journal of Engineering Mechanics 102*, pp. 249–263, 1976.

[10] J. Song and A. Kiureghian, "Generalized bouc-wen model for highly asymmetric hysteresis," *Journal of Engineering Mechanics 132*, pp. 610–618, 2006.

[11] D. Kleinman, "On an iterative technique for riccati equation computations," *IEEE Trans. Autom. Control*, vol. 13, no. 2, pp. 114–115, February 1968.

[12] B. Friedland, *Advanced Control System Design*. Prentice-Hall, 1996.